Generation Mechanism of Carbon Cluster, Fullerene, and Metallofullerene

Shigeo Maruyama

Engineering Research Institute and Department of Mechanical Engineering,
The University of Tokyo
2-11-16 Yayoi, Bunkyo-ku, Tokyo 113-8656, Japan
e-mail: maruyama@photon.t.u-tokyo.ac.jp
URL: http://www.photon.t.u-tokyo.ac.jp/~maruyama

Abstract:

The formation mechanism of empty and metal-containing fullerene was studied through molecular dynamics simulations and Fourier Transform Ion Cyclotron Resonance (FT-ICR) mass spectroscopy of laser vaporized carbon cluster. With classical molecular dynamics simulations using modified Brenner potential, the clustering process starting from 500 isolated carbon atoms in gas phase was simulated under the controlled temperature condition. When the control temperature was at T_c = 3000 K, imperfect caged clusters like C_{60} and C_{70} were obtained. Additional annealing simulations to compensate the short time-scale of the simulation resulted the perfect I_h-C_{60} structure through Stone-Wales transformations. A fullerene formation model featuring the random caged structure and annealing at the size range of C_{40} to C_{60} was proposed through the detailed study of the precursor structures in simulations.

In order to incorporate metal atoms in the simulation, multi-body classical potential functions for metal-carbon and metal-metal interactions were constructed based on DFT (density functional theory) calculations of various forms of small clusters MC_n and M_n (M = La, Sc, Ni). The classical potential was expressed with the Morse term and the Coulomb term as function of coordinate number of a metal atom. The simulated clustering process with addition of 1 % of metal atoms was compared with the pure carbon simulation. When La atoms were applied, the stable open-cap structure surrounding the La atom resulted in the La-containing caged cluster. For Sc-C system, the host carbon clusters were not affected so much as the La-C case due to the weaker Coulomb interaction, and the Sc atom was encapsulated in the host cage at the final stage of the growth process. Ni-C system was also simulated to explore the possible role of metal atoms in the generation of SWNT. The precursor clusters were similar to those in Sc-C system, although the Ni atom finally stayed on a face of 7 or 8 member-ring of the caged structure.

Fourier Transform Ion Cyclotron Resonance (FT-ICR) mass spectrometer directly connected to the laser vaporization cluster beam source was implemented to study the clustering process. With increase of cluster nozzle pressure, three different types of positive mass spectra were obtained for pure carbon clusters: smaller than about C_{60} with odd numbered clusters up to C_{40}; almost only C_{60} and a trace of C_{70}; well-known even atom mass with intense peaks at C_{60} and C_{70}. Qualitatively the lower pressure condition of the cluster source corresponded to the earlier stage of the MD simulation. Through these comparisons, we speculated that the even-numbered clusters

corresponded to the annealed random caged clusters. The FT-ICR mass spectra of metal-carbon binary clusters were studied for sample materials normally used for generation of metal-containing fullerene and SWNT; La: 0.8%, Y: 0.8%, Sc: 0.8%, Gd: 0.8%, Ce: 0.8%, Ca: 0.3%, and Ni:4.2% - Y: 1%. Positive La-C, Y-C, Sc-C, Gd-C, Ce-C binary clusters commonly showed strong MC_{2n}^{+} signal in the range of $36 < 2n < 76$ with intense magic numbers at MC_{44}^{+}, MC_{50}^{+} and MC_{60}^{+}. Characteristics of these small clusters were compared with results of molecular dynamics simulations.

In order to further study the information of clusters appearing in the mass spectra, reactivity of negative carbon clusters and metal-carbon binary clusters to NO were measured by the FT-ICR spectrometer. For empty clusters, even-odd alternation of reactivity was clearly shown; even clusters were less reactive. Furthermore, carbon clusters with La atom such as LaC_{44}^{-} were very much unreactive to NO. The reactivity of clusters contaminated with a hydrogen atom was very curious. One hydrogen atom made odd-numbered clusters less reactive and even-numbered clusters more reactive. These experimental results were perfectly explained by a consideration of number of dangling bonds based on the random-raged geometric structure predicted by the molecular dynamics simulations.

Int. Symp. Micro/Nano Scale Mech. Eng.
Dec. 1999, Seoul University

Generation Mechanism of Carbon Cluster, Fullerene, and Metallofullerene

Shigeo Maruyama

Engineering Research Institute
& Department of Mechanical Engineering
The University of Tokyo
e-mail: maruyama@photon.t.u-tokyo.ac.jp
URL: http://www.photon.t.u-tokyo.ac.jp/~maruyama
Co-Workers:
Masamichi Kohno, Shuhei Inoue, Tetsuya Yoshida,
Hideaki Hayashi, and Yasutaka Yamaguchi

Current Research Projects

	Experimental	Molecular Dynamics Simulations
Fullerene & Carbon Nanotube	➢Laser-Vap. Cluster Source + FT-ICR Mass Spectrometry + Time of Flight ➢Arc-Discharge Generator ➢Laser-Oven Generator (SWNT)	➢Fullerene Formation Mechanism ➢Metal-Containing Fullerene ➢Hydrogen Storage by SWNT
Silicon Clusters, Surface & Bulk	➢Photo-Fragmentation in TOF ➢Chemical Reaction in FT-ICR ➢Quantum Dots?	➢Tight-Binding and Quantum MD ➢Dissociation Dynamics ➢Phase Change (Polycrystalline)
Inter-Phase Phenomena		➢Liquid Droplet on Solid Surface ➢Vapor Bubble Nucleation ➢Droplet and Surface Tension ➢Thermal Boundary Resistance
Light-Matter Interaction	➢Laser Annealing of Clusters ➢Photo-Fragmentation	➢Non-Adiabatic MD?

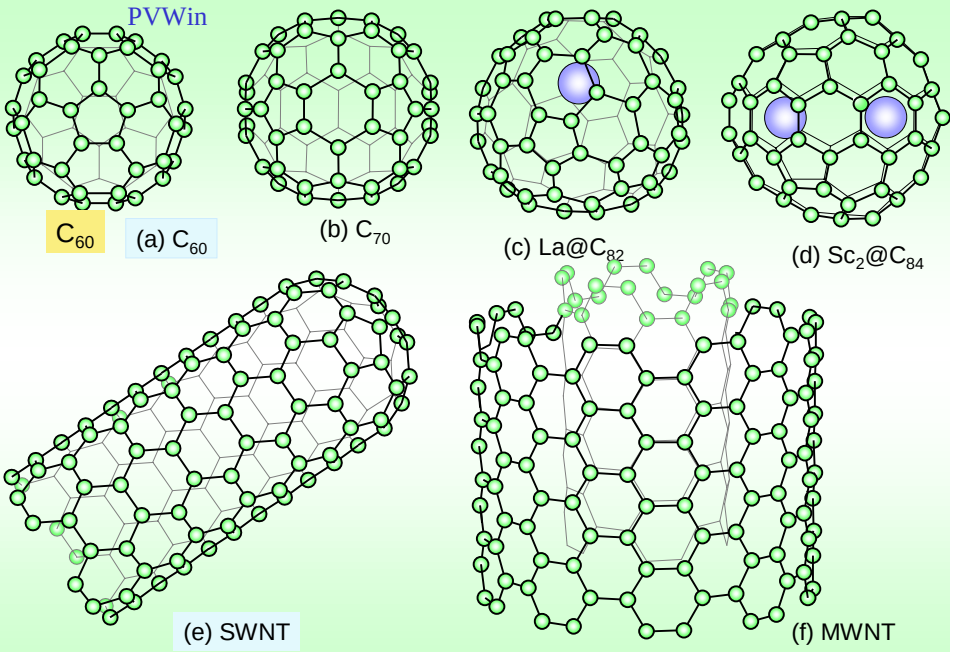

Typical Structures of Fullerene

Total Energy E_b:

Molecular Dynamics Simulation
C-C Potential Function

$$E_b = \sum_i \sum_{j(<i)} \{V_R(r_{ij}) - B^*_{ij} V_A(r_{ij})\}$$

$$V_R(r) = f(r)\frac{D_e}{S-1}\exp\{-\beta\sqrt{2S}(r-R_e)\} \qquad V_A(r) = f(r)\frac{D_e S}{S-1}\exp\left\{-\beta\sqrt{\frac{2}{S}}(r-R_e)\right\}$$

$$B^*_{ij} = \frac{B_{ij}+B_{ji}}{2}, \quad B_{ij} = \left[1+\sum_{k(\neq i,j)}\{G_c(\theta_{ijk})f(r_{ik})\}\right]^{-\delta}$$

Cut-off function

$$G_c(\theta) = a_0\left(1+\frac{c_0^2}{d_0^2}-\frac{c_0^2}{d_0^2+(1+\cos\theta)^2}\right)$$

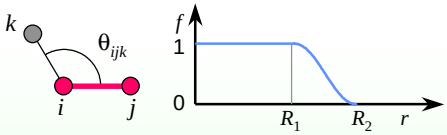

Potential parameters

$D_e =$	6.325 eV	$S =$	1.29	$\beta =$	1.5 Å^{-1}	$R_e =$	1.315 Å
$\delta =$	0.80469	$a_0 =$	0.011304	$c_0 =$	19	$d_0 =$	2.5
$R_1 =$	1.7 Å	$R_2 =$	2.0 Å				

From D. W. Brenner: *Phys. Rev. B*, **42**, 9458(1990)

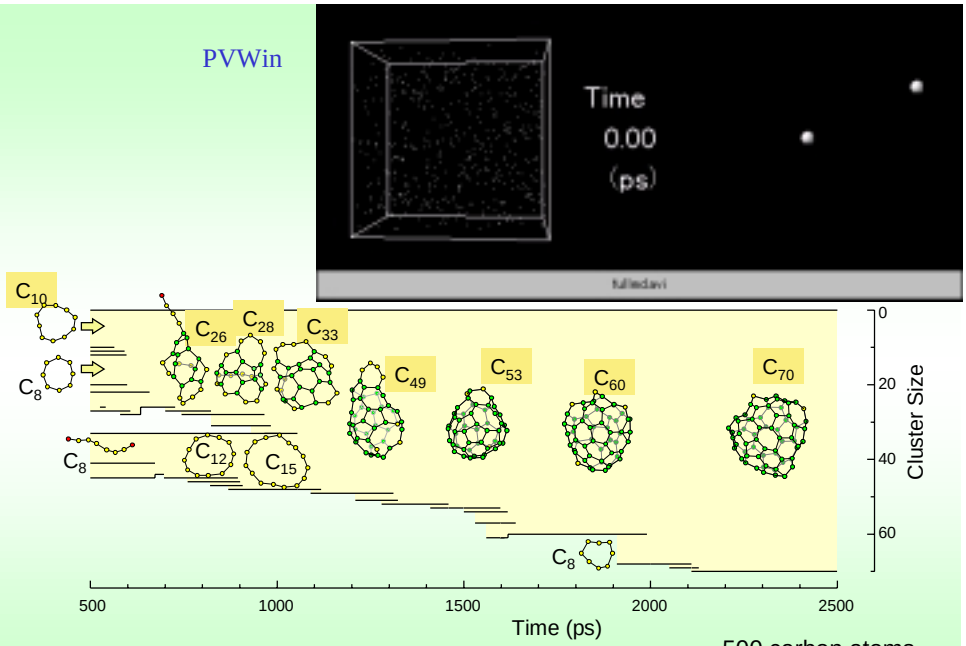
PVWin
Time
0.00
(ps)
C10
C8
C26
C28
C33
C49
C53
C60
C70
C8
C12
C15
C8
0
20
40
60
Cluster Size
500
1000
1500
2000
2500
Time (ps)
Growth Process
500 carbon atoms
342 Å cubic box
T_c = 3000 K

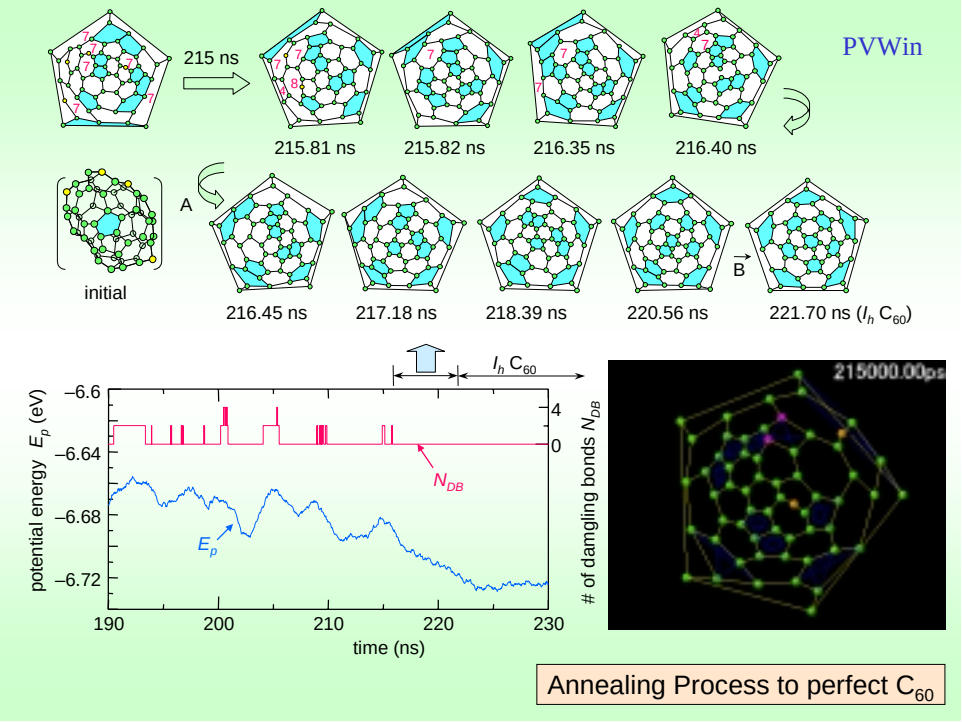
PVWin
215 ns
215.81 ns
215.82 ns
216.35 ns
216.40 ns
initial
A
B
216.45 ns
217.18 ns
218.39 ns
220.56 ns
221.70 ns (I_h C_{60})
I_h C_{60}
potential energy E_p (eV)
−6.6
−6.64
−6.68
−6.72
N_{DB}
E_p
4
0
# of dangling bonds N_{DB}
190
200
210
220
230
time (ns)
215000.00ps
Annealing Process to perfect C_{60}

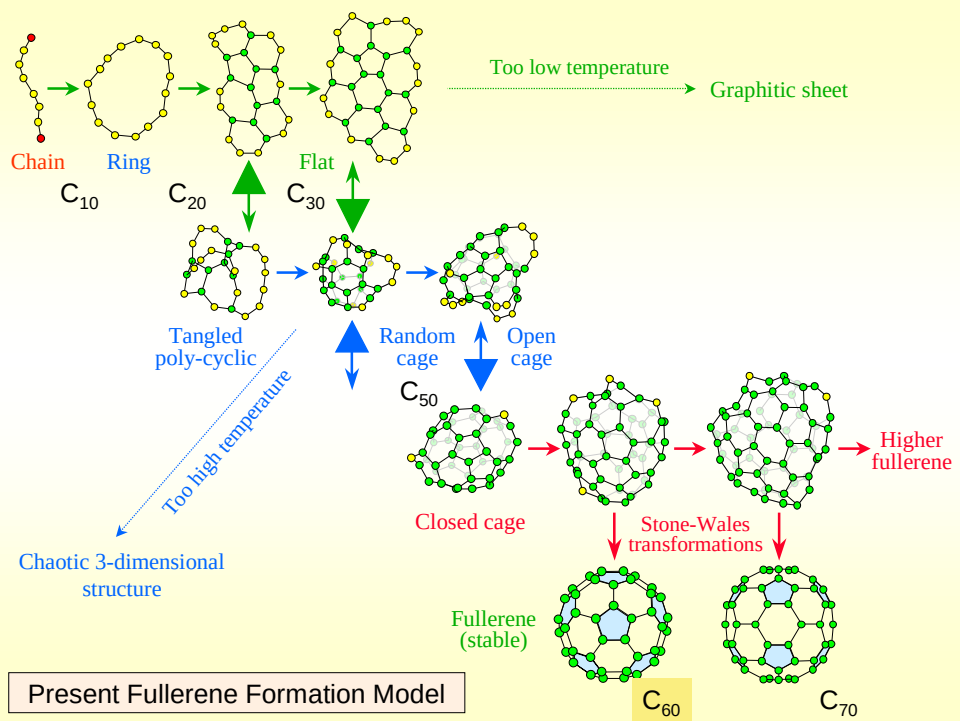

Present Fullerene Formation Model

Group	1	2	3	4	5	6	7	8	9	10	11	12	13	14	15	16	17	18
Period																		
1	1 H 1.008																	2 He 4.003
2	3 Li 6.941	4 Be 9.012											5 B 10.81	6 C 12.01	7 N 14.01	8 O 16.00	9 F 19.00	10 Ne 20.18
3	11 Na 22.99	12 Mg 24.31											13 Al 26.98	14 Si 28.09	15 P 30.97	16 S 32.07	17 Cl 35.45	18 Ar 39.95
4	19 K 39.10	20 Ca 40.08	21 Sc 44.96	22 Ti 47.88	23 V 50.94	24 Cr 52.00	25 Mn 54.94	26 Fe 55.85	27 Co 58.93	28 Ni 58.69	29 Cu 63.55	30 Zn 65.39	31 Ga 69.72	32 Ge 72.61	33 As 74.92	34 Se 78.96	35 Br 79.90	36 Kr 83.80
5	37 Rb 85.47	38 Sr 87.62	39 Y 88.91	40 Zr 91.22	41 Nb 92.91	42 Mo 95.94	43 Tc 99.00	44 Ru 101.1	45 Rh 102.9	46 Pd 106.4	47 Ag 107.9	48 Cd 112.4	49 In 114.8	50 Sn 118.7	51 Sb 121.8	52 Te 127.6	53 I 126.9	54 Xe 131.3
6	55 Cs 132.9	56 Ba 137.3	*	72 Hf 178.5	73 Ta 180.9	74 W 183.8	75 Re 186.2	76 Os 190.2	77 Ir 192.2	78 Pt 195.1	79 Au 197.0	80 Hg 200.6	81 Tl 204.4	82 Pb 207.2	83 Bi 209.0	84 Po 210.0	85 At 210.0	86 Rn 222.0
7	87 Fr 223	88 Ra 226	**	104 Unq 261	105 Unp 262	106 Unh 263	107 Uns 262	108 Uno 265	109 Une 266	110 Uun 269	111 Uuu 272	112 Uub 277						
–																		
* Lanthanides			57 La 138.9	58 Ce 140.1	59 Pr 140.9	60 Nd 144.2	61 Pm 145	62 Sm 150.4	63 Eu 152	64 Gd 157.3	65 Tb 158.9	66 Dy 162.5	67 Ho 164.9	68 Er 167.3	69 Tm 168.9	70 Yb 173.0	71 Lu 175.0	
** Actinides			89 Ac 227	90 Th 232	91 Pa 231	92 U 238	93 Np 237	94 Pu 239	95 Am 243	96 Cm 247	97 Bk 247	98 Cf 252	99 Es 252	100 Fm 257	101 Md 258	102 No 259	103 Lr 262	

Studied Metal Atoms

$E_{ij} = V_R + V_A + V_C$

$f(r_{ij})$: cut-off function

V_R: Repulsive term

$$V_R = f(r_{ij})\frac{D_e}{S-1}\exp\left\{-\beta\sqrt{2S}(r_{ij}-R_e)\right\}$$

V_A: Attractive term

$$V_A = -f(r_{ij})\cdot B^*\frac{D_e S}{S-1}\exp\left\{-\beta\sqrt{2/S}(r_{ij}-R_e)\right\}$$

M-C

B^*: normalized bond order

$$B^* = \left\{1+b(N^{\mathrm{C}}-1)\right\}^{\delta}$$

N^{C}: carbon coordinate number

$$N^{\mathrm{C}} = 1+\sum_{\text{carbon } k(\neq j)} f(r_{ik})$$

V_C: Coulomb term

$$V_C = -f(r_{ij})\frac{e^2}{4\pi\varepsilon_0}\frac{c_{\mathrm{C}}c_{\mathrm{M}}}{r_{ij}}$$

c_{M}, c_{C} : charge of M (+) and C(-)

$$c_{\mathrm{M}} = 3-\exp(-k_1 N^{\mathrm{C}}+k_2) \qquad c_{\mathrm{C}} = c_{\mathrm{M}}/N^{\mathrm{C}}$$

M-M

$$R_e(N_{ij}) = R_{e1}-R_{e2}\exp\left\{-C_R(N_{ij}-1)\right\}$$

$$D_e(N_{ij}) = D_{e1}+D_{e2}\exp\left\{-C_D(N_{ij}-1)\right\}$$

$N^{\mathrm{M}}{}_i$: metal coordinate number

$$N^{\mathrm{M}}{}_i = 1+\sum_{\text{metal } k(\neq j)} f(r_{ik}) \qquad N_{ij} = \frac{N^{\mathrm{M}}{}_i + N^{\mathrm{M}}{}_j}{2}$$

$$V_C = f(r_{ij})\frac{e^2}{4\pi\varepsilon_0}\frac{c_{\mathrm{M}i}c_{\mathrm{M}j}}{r_{ij}}$$

M-C and M-M Potential Function Expression

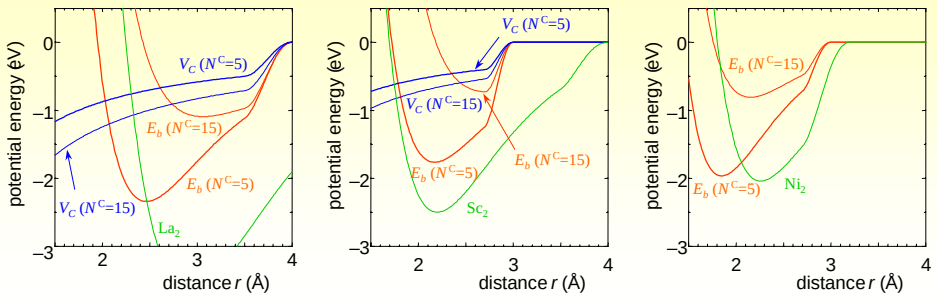

(a) La-C (b) Sc-C (c) Ni-C

Table 1. Potential parameters for metal-carbon interactions.

	D_e (eV)	S	β (1/Å)	R_e (Å)	R_1 (Å)	R_2 (Å)	b	δ	k_1	k_2
La-C	4.53	1.3	1.5	2.08	3.2	3.5	0.0854	-0.8	0.0469	1.032
Sc-C	3.82	1.3	1.7	1.80	2.7	3.0	0.0936	-0.8	0.0300	1.020
Ni-C	3.02	1.3	1.8	1.70	2.7	3.0	0.0330	-0.8	–	–

Table 2. Potential parameters for metal-metal interactions.

	S	β (1/Å)	D_{e1} (eV)	D_{e2} (eV)	C_D	R_{e1} (Å)	R_{e2} (Å)	C_R	R_1 (Å)	R_2 (Å)
La-La	1.3	1.05	0.740	2.64	0.570	3.735	0.777	0.459	4.0	4.5
Sc-Sc	1.3	1.4	0.645	1.77	0.534	3.251	0.919	0.620	3.5	4.0
Ni-Ni	1.3	1.55	0.74	1.423	0.365	2.520	0.304	0.200	2.7	3.2

Metal-Carbon Potential functions

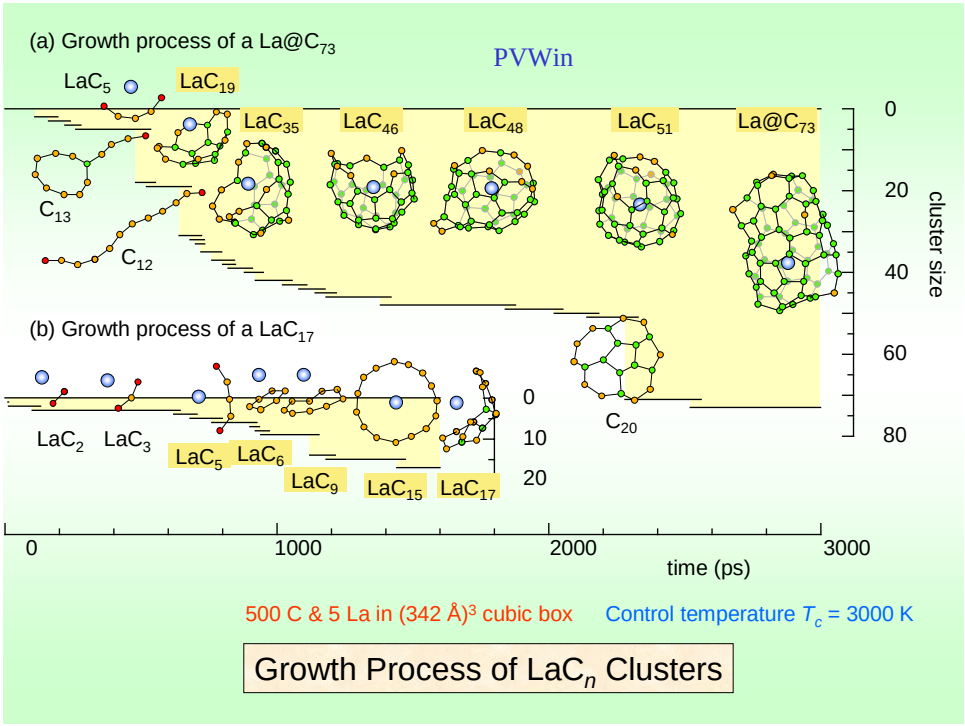

Growth Process of LaC_n Clusters

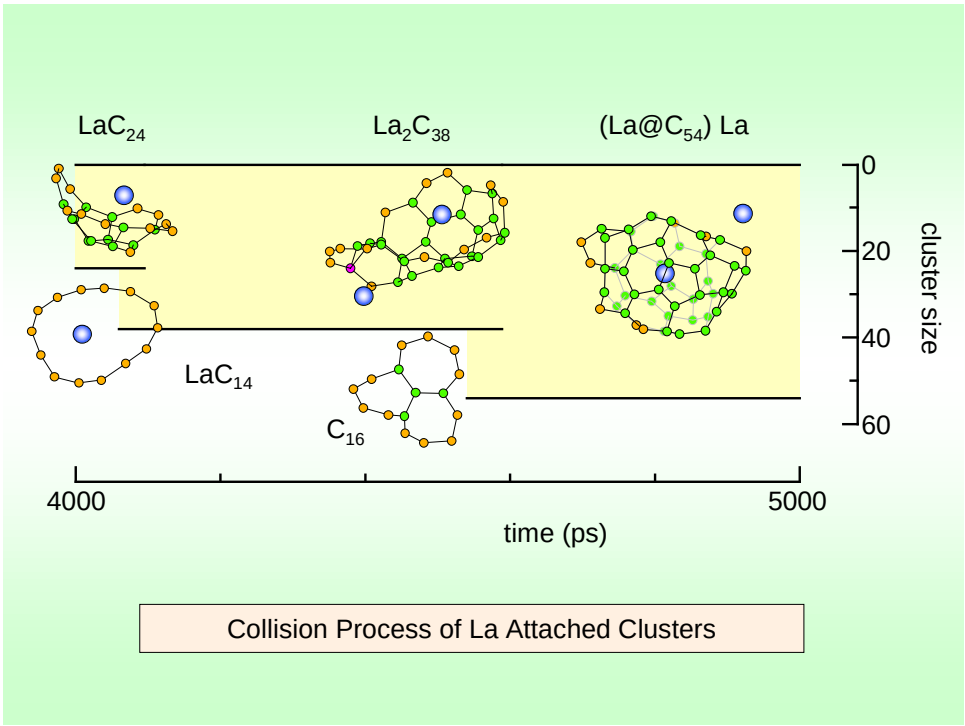

Collision Process of La Attached Clusters

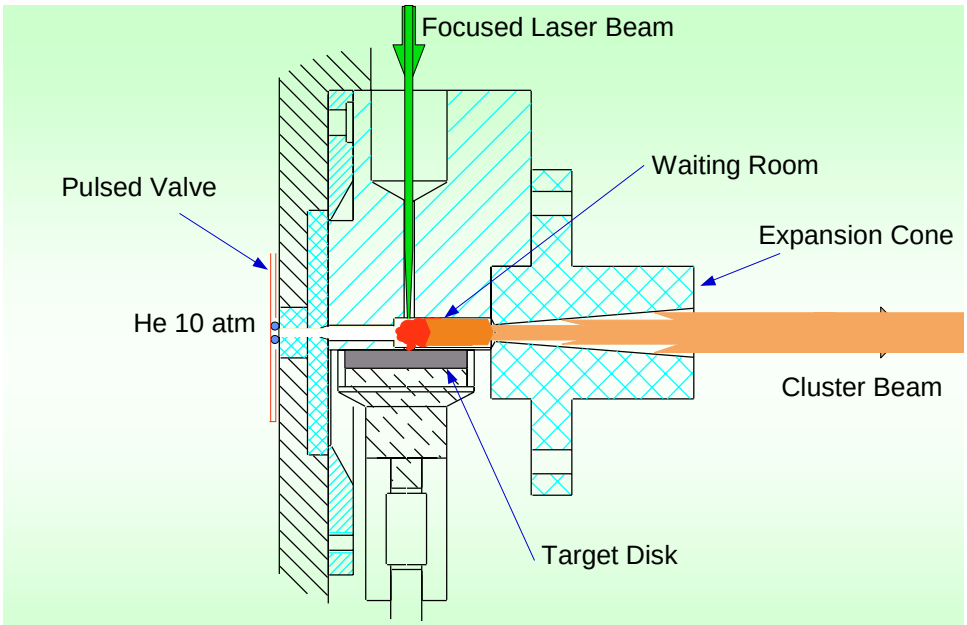

Cluster Source Nozzle for FT-ICR

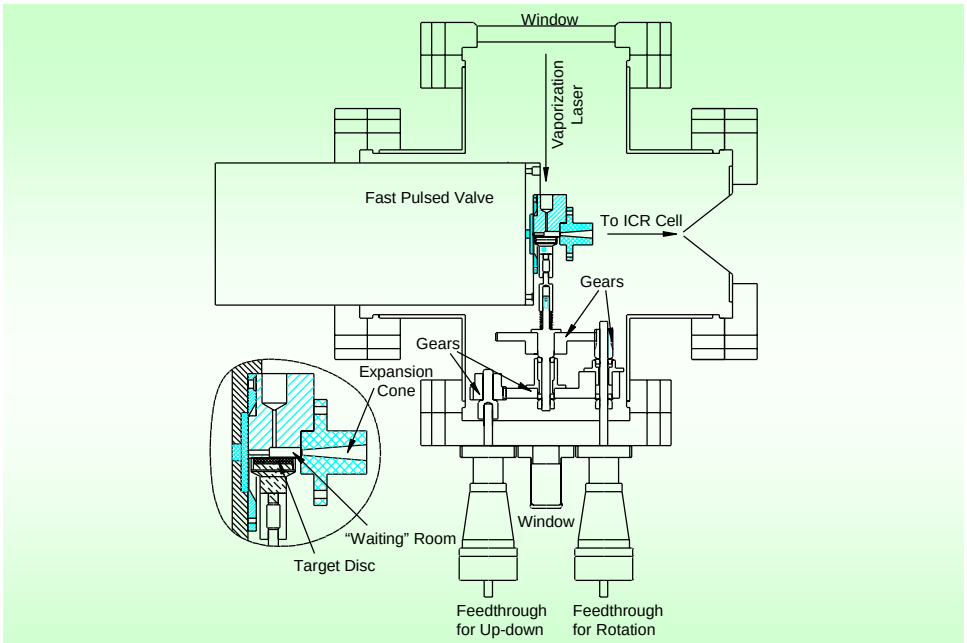

Cluster Source for FT-ICR

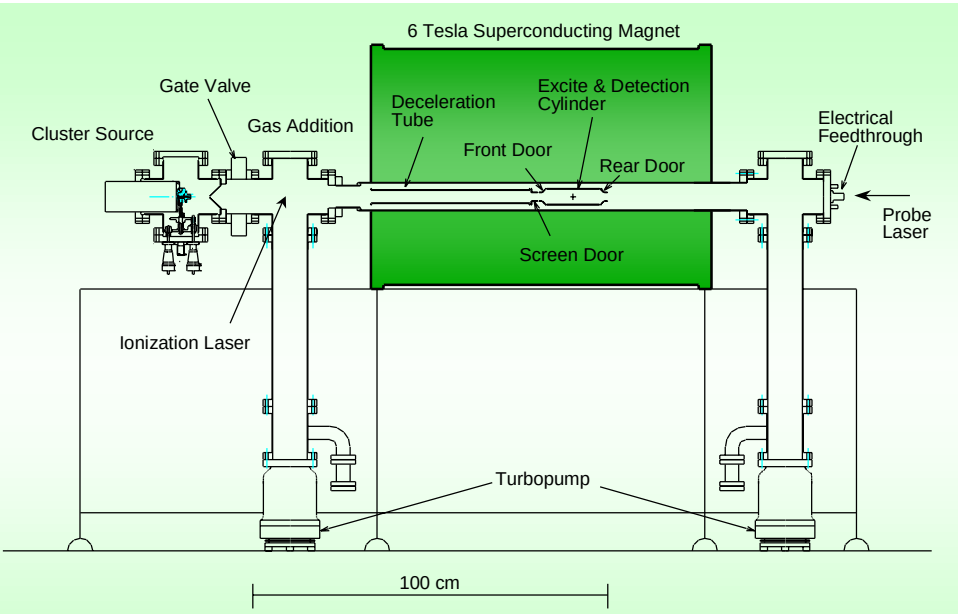

FT-ICR (Fourier Transform Ion Cyclotron Resonance) Mass Spectrometer

$$F = qvB = \frac{mv^2}{r}$$

$$f = \frac{v}{2\pi r} = \frac{qB}{2\pi m}$$

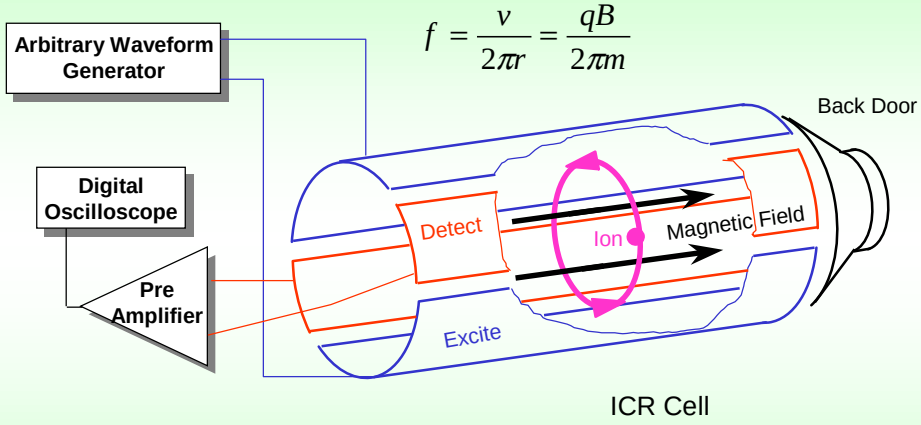

Mechanism of Fourier Transform Ion Cyclotron Resonance Mass Spectrometry (FT-ICR)

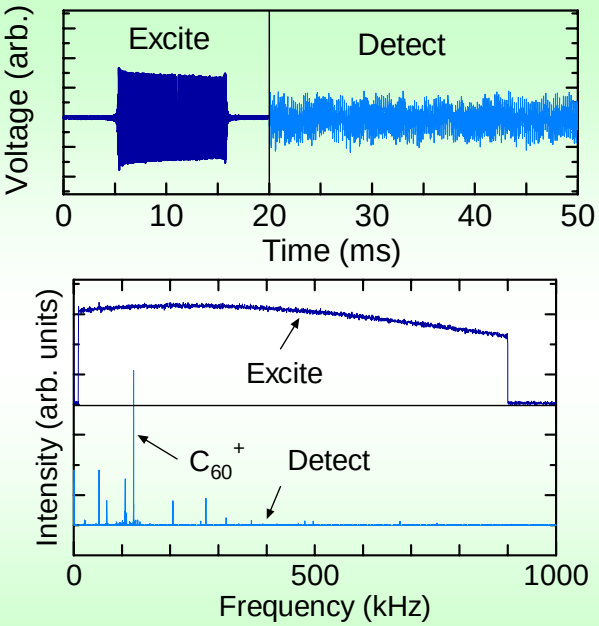

Example of Excite and Detect Waveform

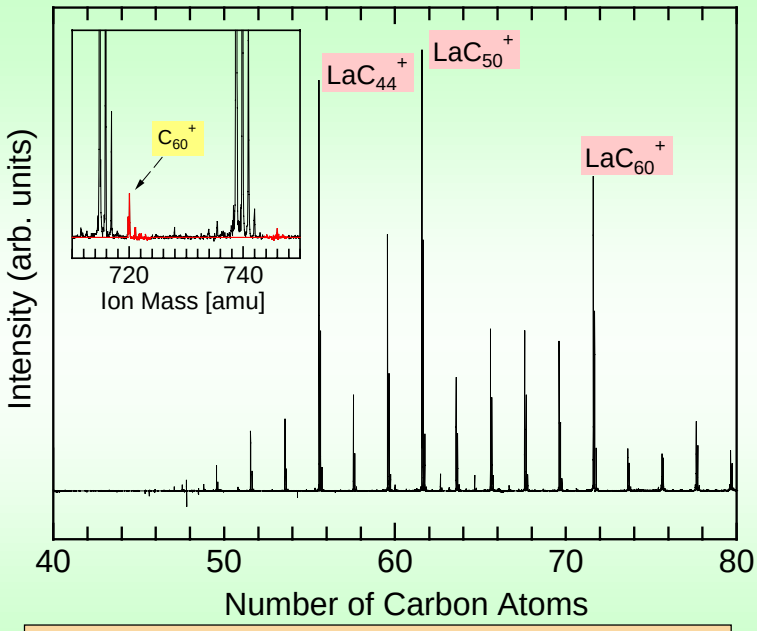

Lanthanum-carbon binary clusters

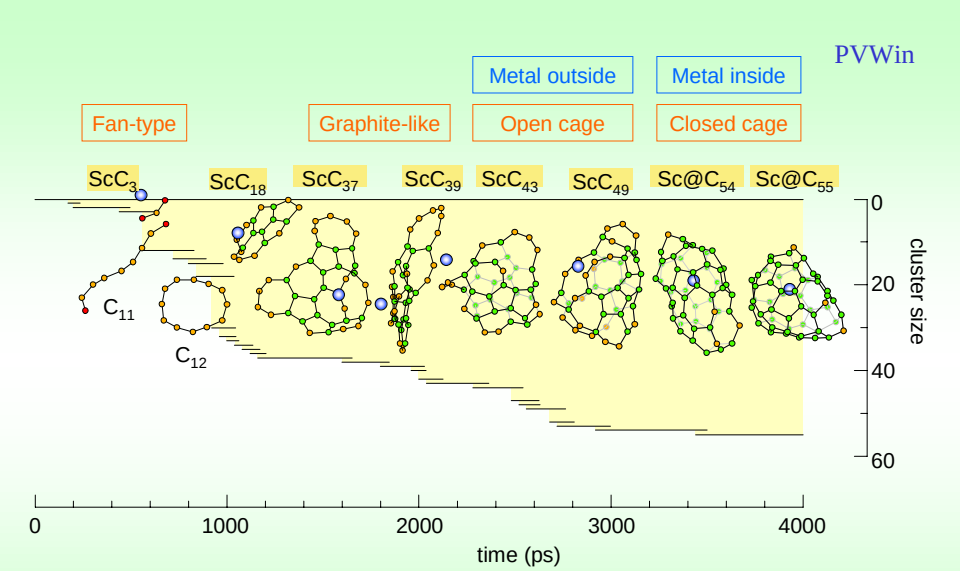

Sc: 5, C: 500 in 34.2nm box

Growth Process of a Sc Containing Cluster

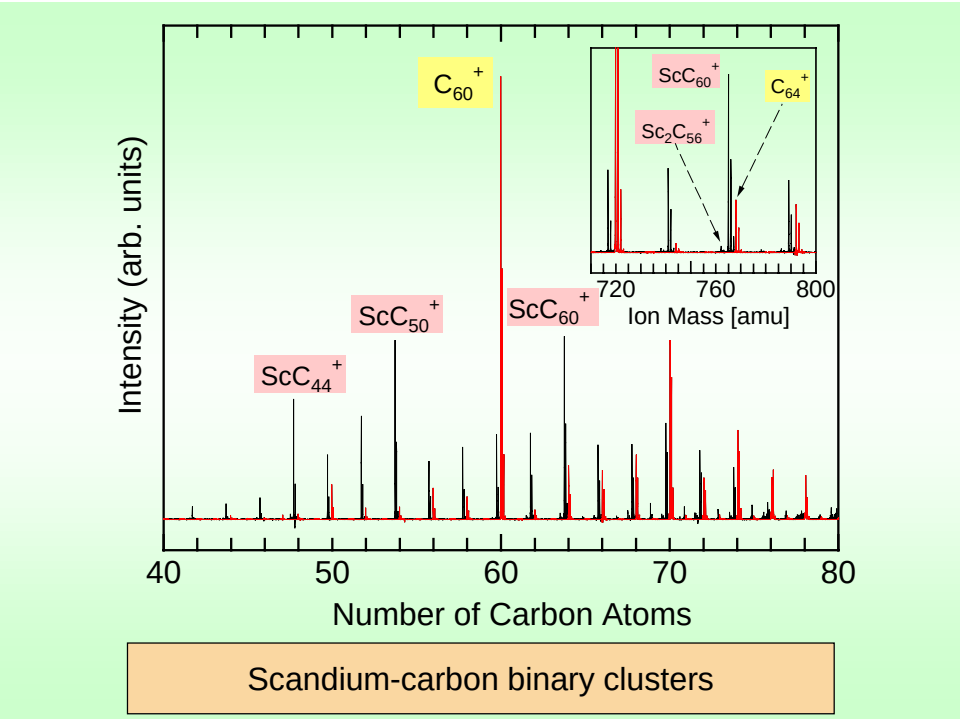

Scandium-carbon binary clusters

Combination of Metals: Ni-Co or Ni-Y is necessary for Production of Single Wall Nanotube

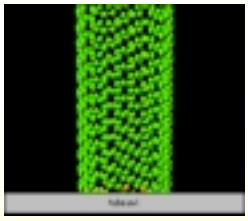

For Production of Single Wall Nanotube (SWNT)

TEM Pictures of SWNT Ropes

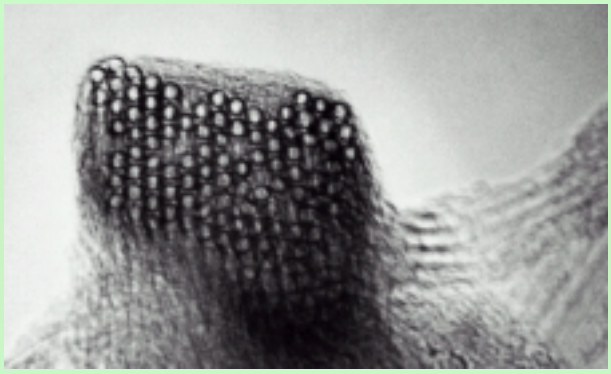

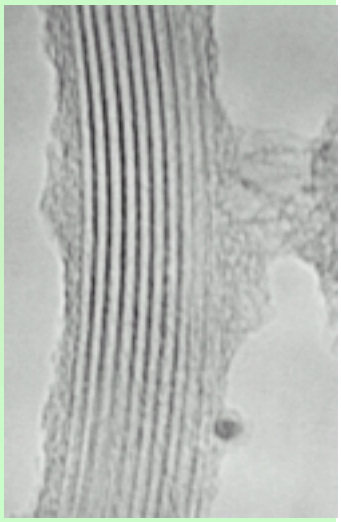

Individual tube diameter: 1.3 nm
Spacing: 0.34 nm
Misalignments and Terminations

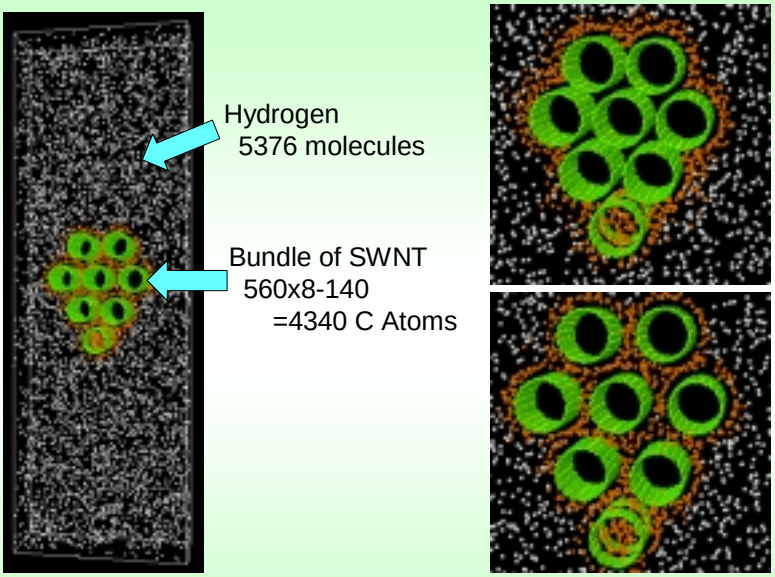

Molecular Simulation of Hydrogen Storage in SWNT

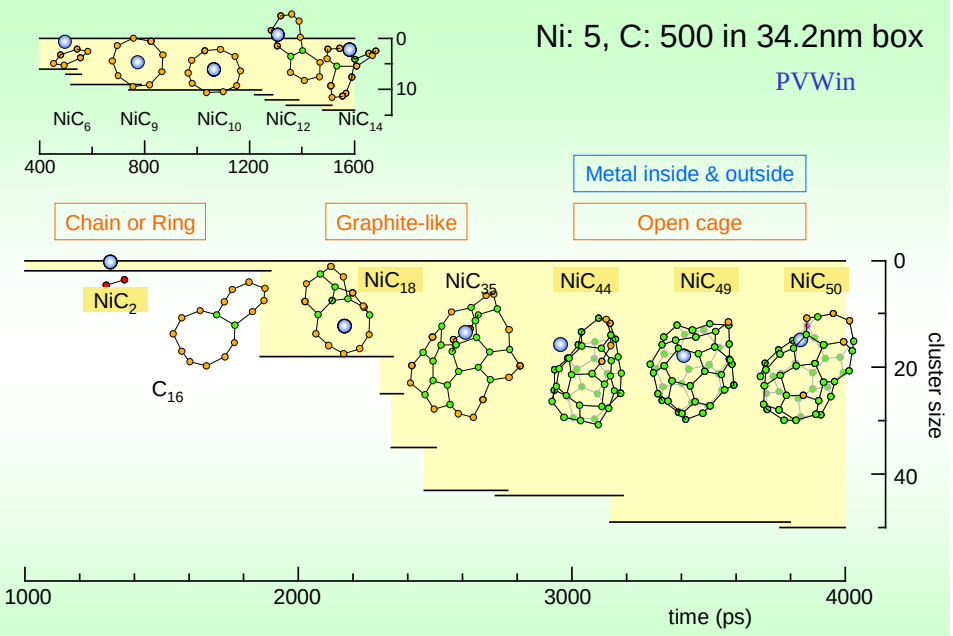

Growth Process of Ni Attached Clusters

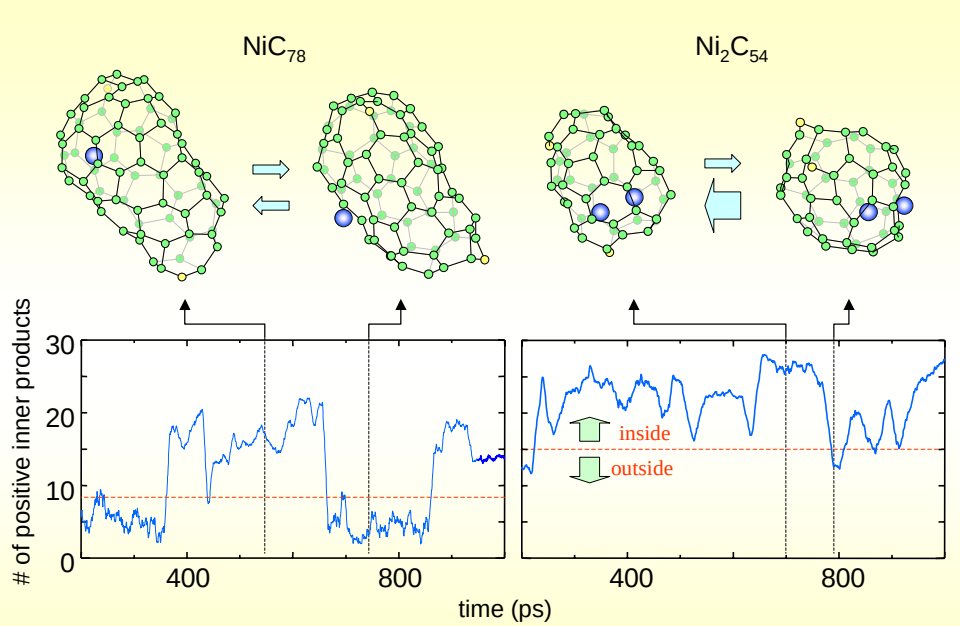

Annealing of NiC_{78} and Ni_2C_{54} Cluster

T_c = 2500 K

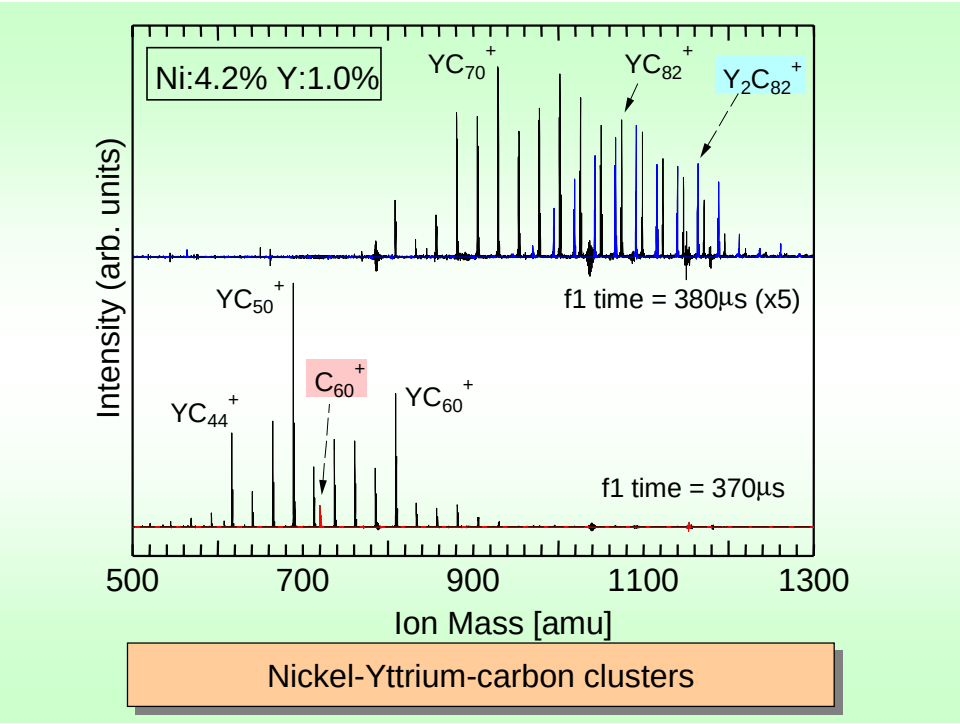

Nickel-Yttrium-carbon clusters

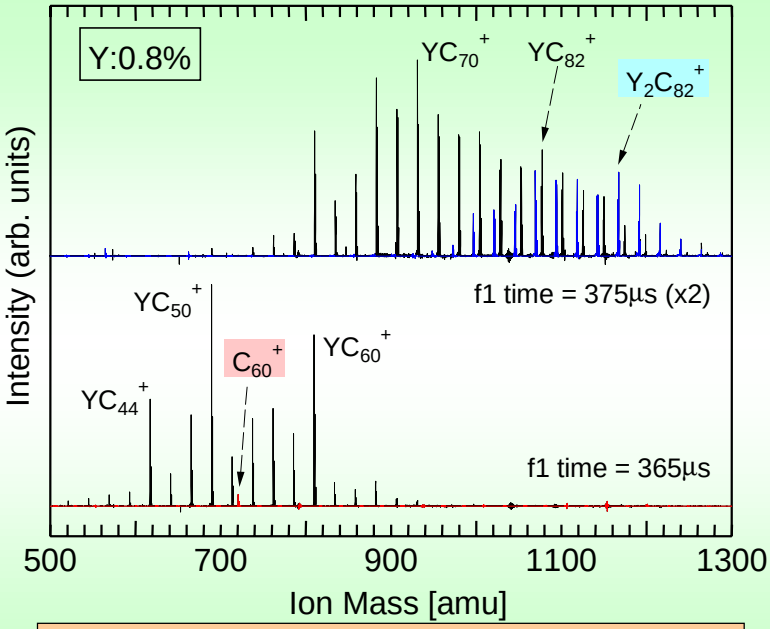

Yttrium-carbon binary clusters

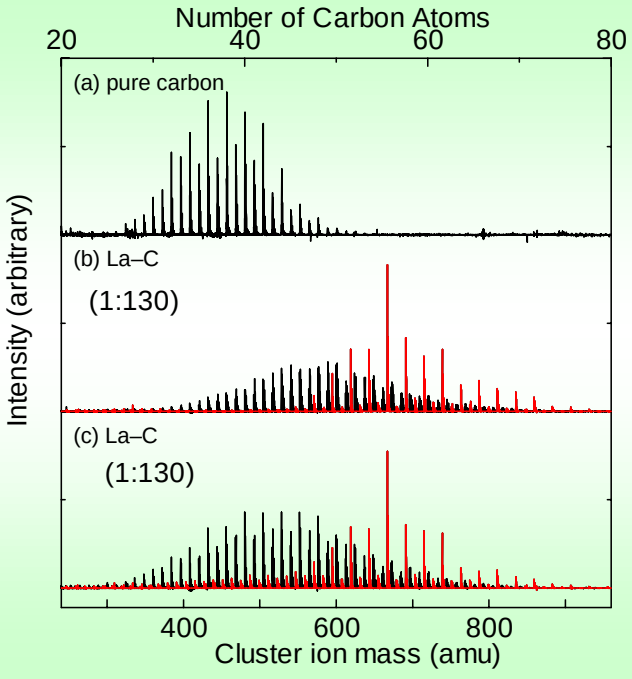

As injected Negative Clusters

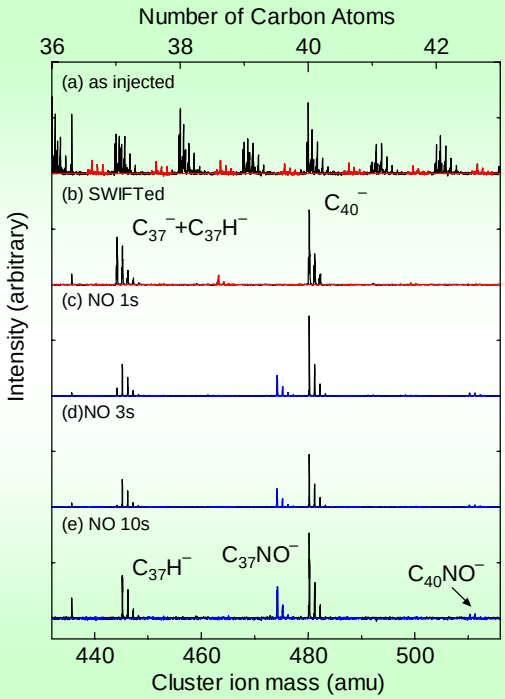

Reaction with NO 10^{-5} Torr

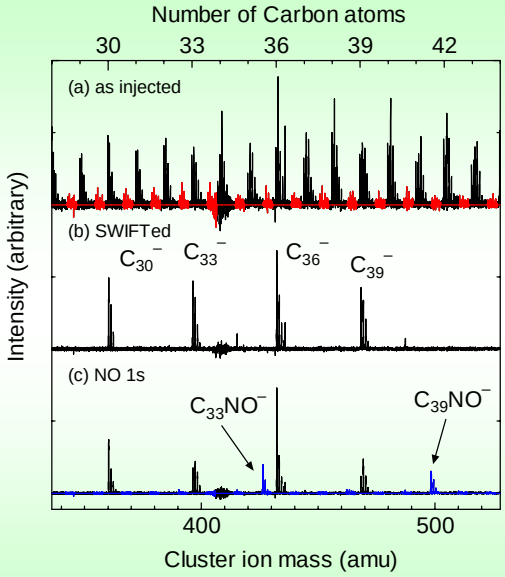

Even-odd Difference of Reactivity for Negative Pure Carbon Cluster

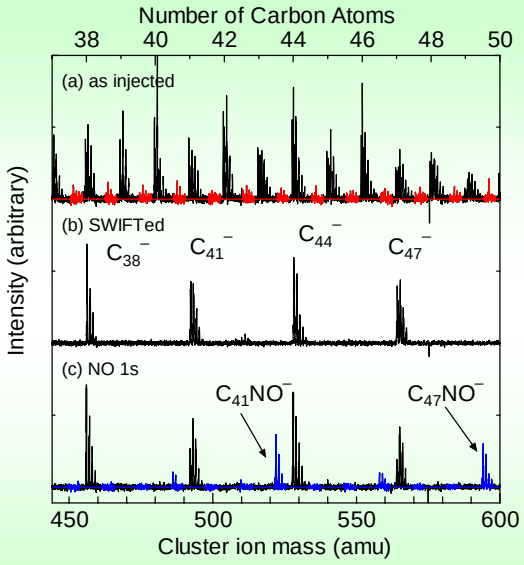

Even-odd Difference of Reactivity for Negative Pure Carbon Cluster

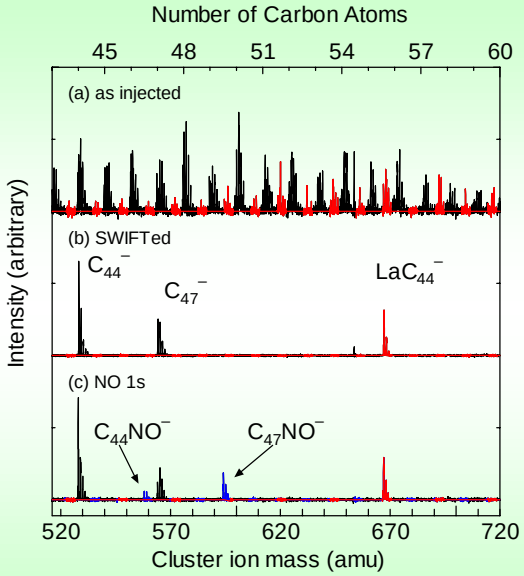

LaC_{44}^- was not Reactive to NO.

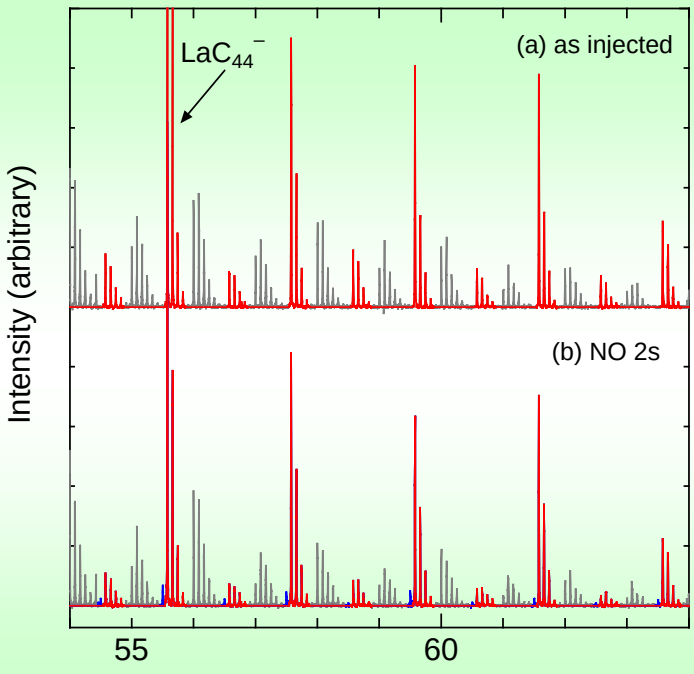

LaC_{odd} Is More Reactive

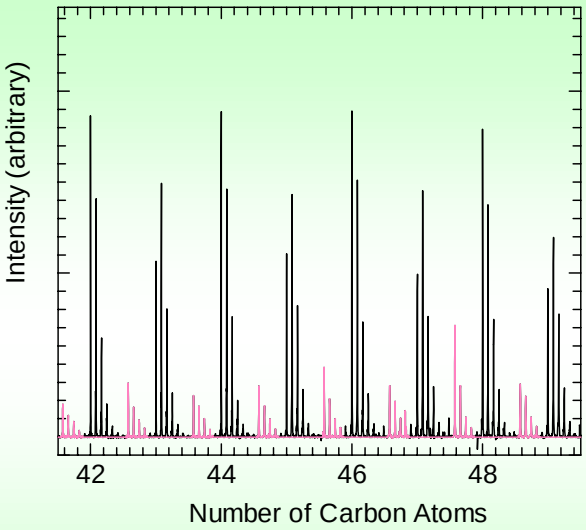

Reaction with H During formation (Dirty Source)

Average of n = 42-51

	C_n	C_nH	C_nH_2	C_nH_3
n: even	71.6%	19.6%	7.2%	1.6%
n: odd	47.0%	43.0%	6.4%	3.6%

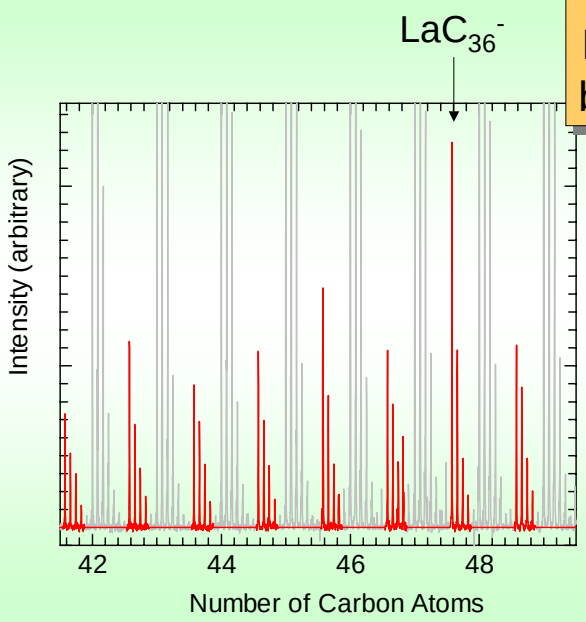

LaC_{36}^- has no Hydrogen Atom by Dirty Source.

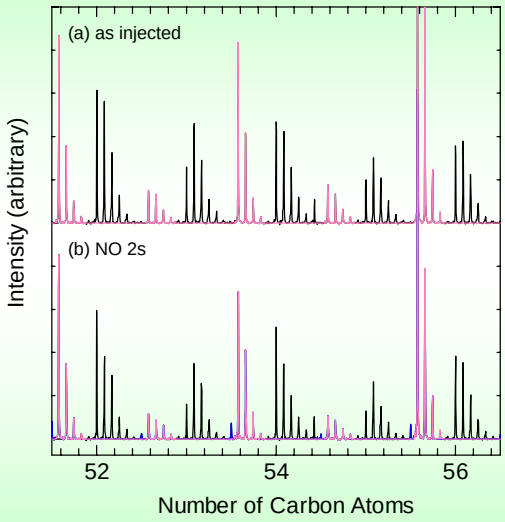

Even Clusters with H Reacts with NO.

Summary for Bare Clusters

Reaction with H (Dirty Source)

Average of n = 42-51

C_{even}: Less Reactive

C_{odd}: More Reactive

	C_n	C_nH	C_nH_2	C_nH_3
n: even	71.6%	19.6%	7.2%	1.6%
n: odd	47.0%	43.0%	6.4%	3.6%

Reaction with NO

C_{even}: Less Reactive

Effect of H: More Reactive $\quad C_{even}H^- + NO \rightarrow \begin{cases} C_{even}HNO^- \\ C_{even}NO^- \end{cases}$

C_{odd}: More Reactive

Effect of H: Unreactive $\quad C_{odd}{}^- + NO \rightarrow C_{odd}NO^-$

Possible Reaction Sites

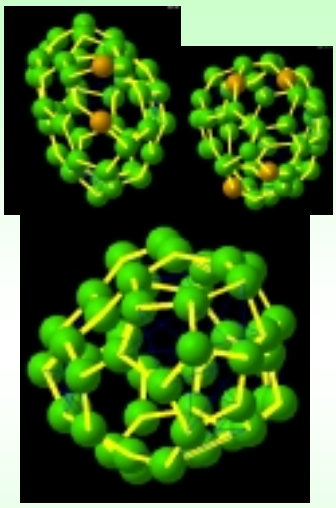

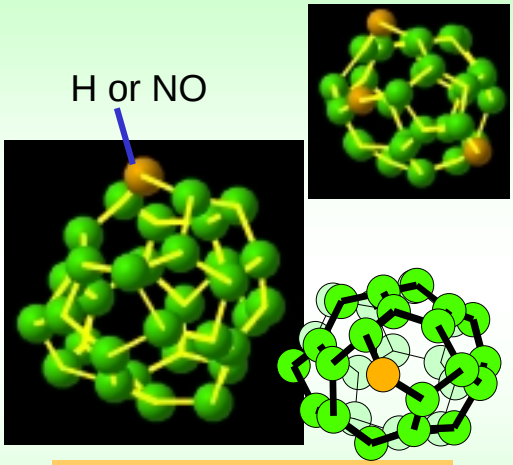

Even Numbered Clusters
# of Dangling Bond = 0, 2, 4, …

Odd Numbered Clusters
# of Dangling Bond = 1, 3, 5, …

Euler's Theorem:

$$f + v = e + 2,\ e = \frac{3}{2}v_3 + v_2,\ f = \frac{v_3}{2} + 2,\ v = v_3 + v_2 = 2f - 4 + v_2$$

Revisit the Use of Euler's Theorem

Euler's Theorem: $f + v = e + 2$

f: faces, *v*: vertices, *e*: edges

Usual Explanation of Even Numbered Positive Spectra

$$f = f_5 + f_6$$

$$\begin{cases} 2e = 5f_5 + 6f_6 \\ 3v = 5f_5 + 6f_6 \end{cases} \Rightarrow \begin{cases} f_5 = 12 \\ v = 20 + 2f_6 \end{cases}$$

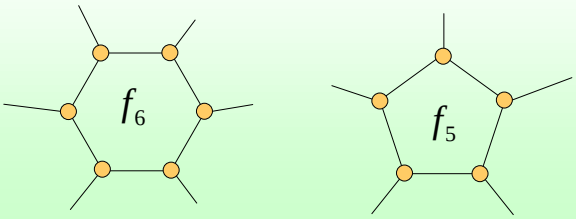

More General Treatment

Euler's Theorem: $f + v = e + 2$

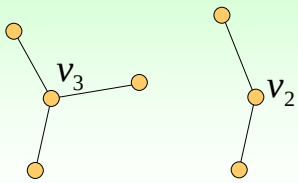

When All Carbon has 3 Bonds

$$e = \frac{3}{2}v \Rightarrow f + v = \frac{3}{2}v + 2 \rightarrow v = 2f - 4$$

v must be even

When Some of Carbon has Dangling Bond

$$e = \frac{3}{2}v_3 + v_2 \Rightarrow f = \frac{v_3}{2} + 2 \rightarrow v = 2f - 4 + v_2$$

$$v = v_3 + v_2$$

v_2 is even/odd when *v* is even/odd

Summary for La-C Binary Clusters

Reaction with H (Dirty Source)

- C_{even}: Less Reactive (less than 10% react) $(n \geq 36)$
- C_{odd}: More Reactive (about 40% react)

Reaction with NO

- C_{even}: Unreactive
- C_{odd}: Reactive

Effect of H: Unreactive

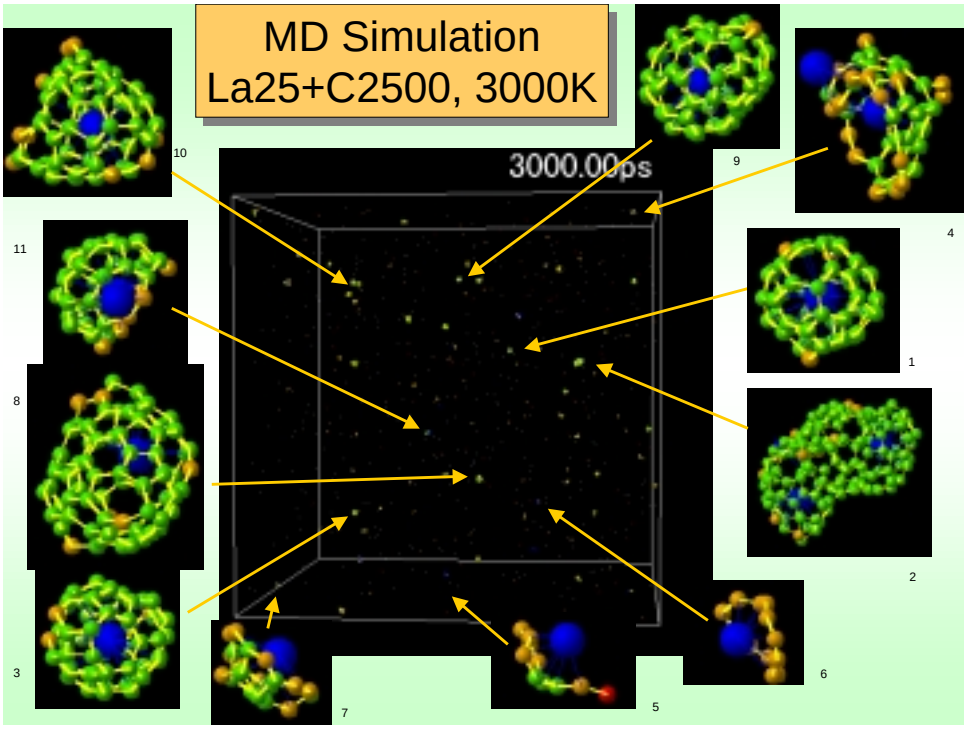

La@C_n Structures (n = Odd) Observed in Molecular Dynamics Simulation

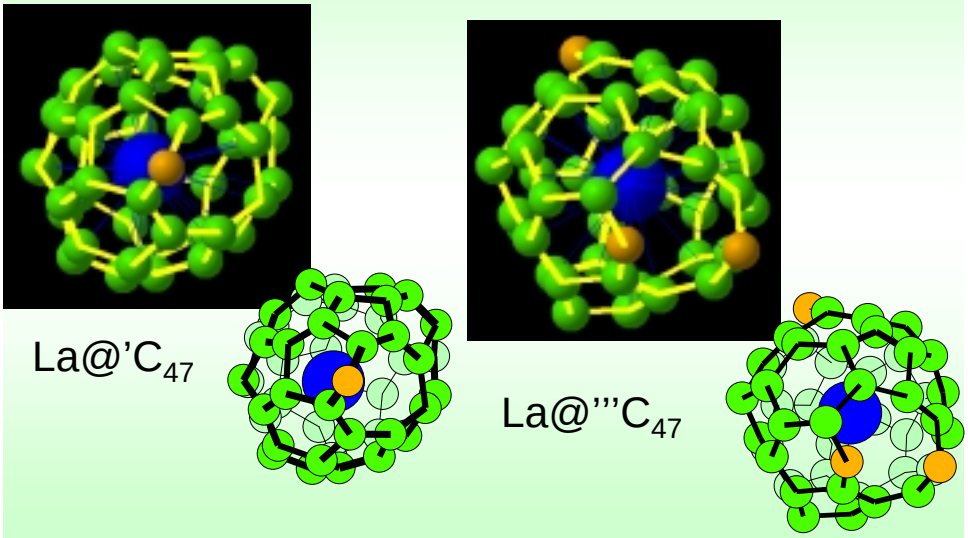

La@C_n Structures (n = Even) Observed in Molecular Dynamics Simulation

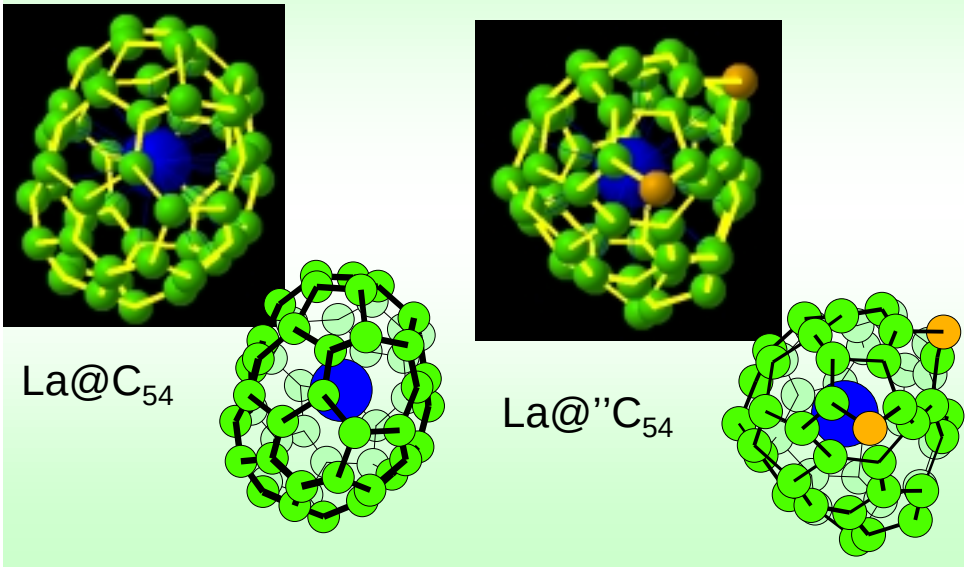

Conclusions

FT-ICR Reaction Results Sugget Annealed Random Cage Model

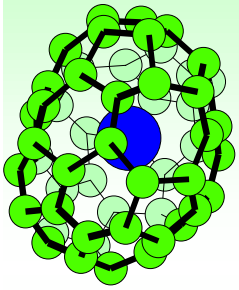

La@C_{even}

@C_{even}

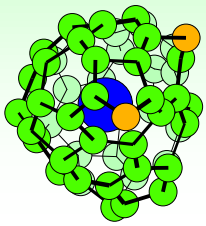

La@''C_{even}

@''C_{even}

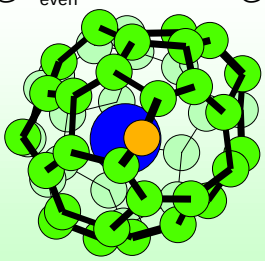

La@'C_{odd}

@'C_{odd}

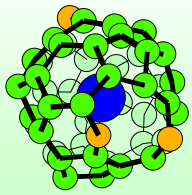

La@'''C_{odd}

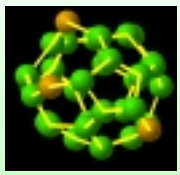

@'''C_{odd}